

## Determination of neutron-induced fission cross-sections of unstable nuclei via surrogate reaction method

B K NAYAK

Nuclear Physics Division, Bhabha Atomic Research Centre, Mumbai 400 085, India  
E-mail: bknayak@barc.gov.in

**DOI:** 10.1007/s12043-014-0874-7; **ePublication:** 4 November 2014

**Abstract.** Heavy ion reaction studies around Coulomb barrier energies have been generally used to investigate the effect of the structure of projectile/target on reaction dynamics. Other than providing an understanding of basic physics of the reaction dynamics, some of these reactions have been used as tools to serve as surrogates of neutron-induced compound nuclear fission cross-sections involving unstable targets. In this paper, we report some of the recent results on the determination of neutron-induced fission cross-sections of unstable actinides present in Th–U and U–Pu fuel cycles by surrogate reaction method by employing transfer-induced fission studies with  ${}^6,7\text{Li}$  beams.

**Keywords.** Neutron-induced fission; surrogate reaction.

**PACS Nos** 24.50.+g; 24.87.+y; 25.85.Ec; 28.20.–v

### 1. Introduction

Compound nuclear cross-sections for reactions of neutrons and light charged particles with target nuclei across the isotopic chart, taking place at energies ranging from several keV to tens of MeV, are required for nuclear astrophysics, national security, and nuclear-energy applications [1]. Not all the relevant data can be directly measured in the laboratory or accurately determined by calculations. Direct measurements may encounter a variety of difficulties: many of the nuclei of interest are too difficult to produce with currently available experimental techniques or too short-lived to serve as targets in the present experimental set-up. Also, sufficient flux of neutron beams of the required energy regime is often inaccessible. Therefore, it becomes necessary to develop indirect methods for determining the relevant reaction cross-sections. The surrogate reaction method is such an indirect method which was first used in the 1970s for estimating neutron-induced fission cross-sections [2,3]. In recent years, this method has been recognized as a potentially powerful tool for a wide range of applications that involve compound nuclear reactions. In Bohr's hypothesis, formation and decay of a compound nucleus are considered to be independent of each other. This independence is exploited in the surrogate reaction

approach. The compound nucleus ( $B^*$ ) formed in the reaction of interest ( $a + A \rightarrow B^* \rightarrow c + C$ ) that involves difficult-to-produce targets is produced via an alternative reaction, called a surrogate reaction ( $d + D \rightarrow B^* + b$ ), which involves a stable projectile–target combination ( $d + D$ ) that is experimentally more feasible. The decay of  $B^*$  is observed in coincidence with the outgoing direct reaction particle  $b$ . The measured compound nuclear decay probabilities can then be multiplied by the calculated capture cross-sections for the compound nucleus in the desired reaction to yield the relevant reaction cross-section. In the past, various surrogate reaction methods such as the absolute surrogate method [2–4], the surrogate ratio method (SRM) [5–8], and the hybrid surrogate ratio method (HSRM) [9–11], have been employed to get indirect estimates of the neutron-induced reaction cross-sections of many short-lived target nuclei. In the absolute surrogate method, the measured fission decay probabilities are simply multiplied by the estimated neutron capture cross-sections to deduce the neutron-induced fission cross-section. However, fission decay probability is the ratio of particle-fission coincident events ( $N_{x-f}$ ) to particle single events ( $N_x$ ),  $P_f(E_{ex}) = (N_{x-f}/N_x)$ . The determination of  $P_f(E_{ex})$  relies largely on the accurate determination of the particle singles counts  $N_x$ , which turns out to be the source of largest uncertainty in the absolute surrogate measurement, due to practical problems of target contamination. The shortcomings of the absolute surrogate method have been eliminated in the SRM. In this method the ratio of the fission probabilities of two compound nucleus reactions for the same excitation energy are determined experimentally. Knowing the cross-section for one of the compound nuclear reactions (reference reaction) allows one to extract the other (desired reaction) by using the ratio  $R(E_{ex})$  as follows:

$$\frac{\sigma_f^{n+(A-1) \rightarrow A^*}(E_{ex})_{(desired)}}{\sigma_f^{n+(B-1) \rightarrow B^*}(E_{ex})_{(reference)}} = R(E_{ex})$$

$$= \frac{\sigma_{n+A-1}^{CN}(E_{ex}) P_f^A(E_{ex})}{\sigma_{n+B-1}^{CN}(E_{ex}) P_f^B(E_{ex})}, \quad (1)$$

where  $(P_f^A(E_{ex})/P_f^B(E_{ex}))$  is the ratio of the decay probabilities of the two compound systems at the same excitation energy which is experimentally measured and the ratio of the neutron capture cross-section for the corresponding target nuclei in the neutron-induced reaction at the same excitation energies  $\sigma_{n+A-1}^{CN}(E_{ex})/\sigma_{n+B-1}^{CN}(E_{ex})$  which is calculated by the optical model thereby enabling one to find out the neutron-induced fission cross-section for an unknown system. More recently, the HSRM, which combines the aspects of both absolute surrogate and SRMs, has been developed and employed by Nayak *et al* [9] to determine the  $^{233}\text{Pa}(n, f)$  cross-sections in the equivalent neutron energy range of 11.5–16.5 MeV for the first time. In SRM, the two compound nuclei corresponding to the desired and reference reactions are populated by performing the same surrogate reaction on two different targets, whereas in the HSRM one performs the two surrogate reactions on the same target *in situ* in two different transfer reactions, where two compound nuclei corresponding to the ‘desired reaction’ and the ‘reference reaction’ are populated. The relative fission decay probabilities of the compound nuclei are measured experimentally to determine the cross-sections of the desired compound nuclear reaction by using eq. (1). In the HSRM, thus by taking a ratio of two reactions on the same target, systematic uncertainties due to target thickness, beam current, and dead time in the determination of the

ratio of fission decay probabilities corresponding to the ‘desired’ and ‘reference’ reactions are eliminated [9,12]. In this work, the results on determination of the compound nuclear neutron-induced fission cross-sections for  $^{234}\text{Pa}$  ( $T_{1/2} = 6.7$  h),  $^{239}\text{Np}$  ( $T_{1/2} = 2.36$  d) and  $^{240}\text{Np}$  ( $T_{1/2} = 61.9$  min) short-lived actinides are reported. The  $^{234}\text{Pa}(n, f)$ ,  $^{239}\text{Np}(n, f)$ , and  $^{240}\text{Np}(n, f)$  compound nuclear cross-sections are determined by measuring the ratio of fission decay probabilities in [ $^{232}\text{Th}(^7\text{Li}, \alpha)^{235}\text{Pa}/^{232}\text{Th}(^7\text{Li}, t)^{236}\text{U}$ ], [ $^{238}\text{U}(^6\text{Li}, \alpha)^{240}\text{Np}/^{238}\text{U}(^6\text{Li}, d)^{242}\text{Pu}$ ], and [ $^{238}\text{U}(^7\text{Li}, \alpha)^{241}\text{Np}/^{238}\text{U}(^7\text{Li}, t)^{242}\text{Pu}$ ] transfer reactions, respectively employing the HSRM.

## 2. Experimental details

Experiments were performed using  $^6,^7\text{Li}$  beams obtained from Bhabha Atomic Research Centre–Tata Institute of Fundamental Research (BARC–TIFR) 14-MV Pelletron Accelerator Facility at Mumbai. The two silicon surface barrier  $\Delta E - E$  detector telescopes with  $\Delta E$  detectors of thicknesses 150 and 100  $\mu\text{m}$  and identical  $E$  detectors of 1 mm thickness were mounted on a reaction plane at  $85^\circ$  and  $105^\circ$  angles with respect to the beam direction to identify the projectile-like fragments (PLFs). An aluminium foil of 4.0  $\text{mg}/\text{cm}^2$  thickness was placed in front of each detector telescope to stop the fission fragments, thereby protect the  $\Delta E$  detectors from radiation damage. A large area (450  $\text{mm}^2$ ) solid-state detector was kept at an angle  $160^\circ$  with respect to the beam direction and subtended a solid angle of 63 msr with an angular opening of  $16^\circ$  to detect the fission fragments coincident with PLFs. The telescopes were energy calibrated by using a  $^{228,229}\text{Th}$  alpha source and in an in-beam experiment that made use of the discrete  $\alpha$ -particle peaks corresponding to  $^{15}\text{N}^*$  states in the  $^{12}\text{C}(^7\text{Li}, \alpha)^{15}\text{N}^*$  reaction at an  $^7\text{Li}$  beam energy of 18.0 MeV.

## 3. Determination of $^{234}\text{Pa}(n, f)$ cross-sections

The compound nuclei  $^{235}\text{Pa}$  and  $^{236}\text{U}$  formed *in situ* in  $^{232}\text{Th}(^7\text{Li}, \alpha)^{235}\text{Pa}^*$  and  $^{232}\text{Th}(^7\text{Li}, t)^{236}\text{U}^*$  transfer reactions are identified by the outgoing alpha and triton PLFs, respectively. The ground-state  $Q$ -values ( $Q_{gg}$ ) for the above reactions are 5.642 and  $-7.040$  MeV, respectively.  $^7\text{Li}$  beam energy of  $E_{\text{lab}} = 39.5$  MeV was chosen, so that the  $^{235}\text{Pa}$  and  $^{236}\text{U}$  compound systems are populated at overlapping excitation energies. The excitation energy spectra for the  $^{235}\text{Pa}$  and  $^{236}\text{U}$  compound systems were obtained by employing two-body kinematics for the outgoing PLFs alpha and triton, respectively. The excitation energy spectra of  $^{235}\text{Pa}$  and  $^{236}\text{U}$  compound systems for the PLF-fission coincidence and PLF singles are shown in figure 1.

The fission decay probabilities of  $^{235}\text{Pa}$  and  $^{236}\text{U}$  compound systems were determined in steps of 1.0 MeV excitation energy bin by taking the ratio of the number of coincidence events between the outgoing PLF-fission fragment coincidence to the number of PLF singles, using eq. (2) as follows:

$$P_f^{\text{CN}}(E_{\text{ex}}) = \frac{N_{i-t}(E_{\text{ex}})}{N_i(E_{\text{ex}})}, \quad (2)$$

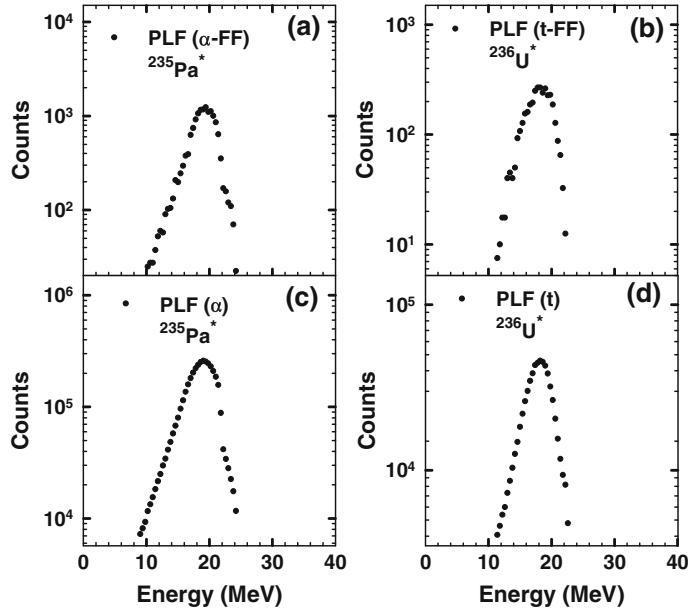


**Figure 1.** Excitation energy spectra of target-like fragments in  ${}^7\text{Li} + {}^{232}\text{Th}$  reaction without (bottom) and with (upper) coincidence with fission fragments.

where  $i$  denotes the alpha or triton PLF channels. For each excitation energy bin of 1.0 MeV, the ratio of fission decay probability of the  ${}^{235}\text{Pa}$  and  ${}^{236}\text{U}$  compound nuclei was determined. The relative fission probabilities of the compound nuclei were then multiplied by the ratio of the corresponding neutron-induced compound nucleus formation cross-section  $\sigma_{n+{}^{234}\text{Pa}}^{\text{CN}}(E_{\text{ex}})$  and  $\sigma_{n+{}^{235}\text{U}}^{\text{CN}}(E_{\text{ex}})$ , to obtain the ratio of the compound nuclear reaction cross-section at the excitation energies of  $n + {}^{234}\text{Pa} \rightarrow {}^{235}\text{Pa} \rightarrow \text{fission}$  and  $n + {}^{235}\text{U} \rightarrow {}^{236}\text{U} \rightarrow \text{fission}$  reaction using eq. (1). The well measured  $n + {}^{235}\text{U} \rightarrow {}^{236}\text{U} \rightarrow \text{fission}$  cross-sections in the 0–30.0 MeV neutron energy range were taken from ENDF/B-VII.1 [13] and used as the reference reaction with energy scale converted to excitation energy by adding the neutron separation energy of  ${}^{236}\text{U}$  ( $S_n = 6.545$  MeV). The neutron-induced compound nuclear formation cross-sections for  ${}^{234}\text{Pa}$  and  ${}^{235}\text{U}$  nuclei have been calculated at the corresponding excitation energies using EMPIRE-3.1 code [14] with optical model potential (OMP) parameters taken from RIPL catalog number 2408 from Capote *et al* [15]. The  ${}^{234}\text{Pa}(n, f)$  cross-sections as a function of excitation energy were obtained over the 14–20 MeV energy range, using eq. (1). Finally, the excitation energies were scaled down by subtracting the  ${}^{235}\text{Pa}$  neutron separation energy ( $S_n = 6.123$ ) to obtain the  ${}^{234}\text{Pa}(n, f)$  cross-sections at the appropriate equivalent neutron energies. The present experimental results for the  ${}^{234}\text{Pa}(n, f)$  cross-sections in the equivalent neutron energy range of 8–14 MeV are shown in figure 2 along with the predictions of EMPIRE-3.1 code for the fission barrier heights obtained from the barrier formula (BF) [9,16,17] and RIPL-3 [18]. The present experimental data agree very well with the calculated neutron-induced fission cross-sections for the fission barrier heights obtained from BF. The predictions of EMPIRE-3.1 for the RIPL-3 fission barriers are in agreement only with the data for the

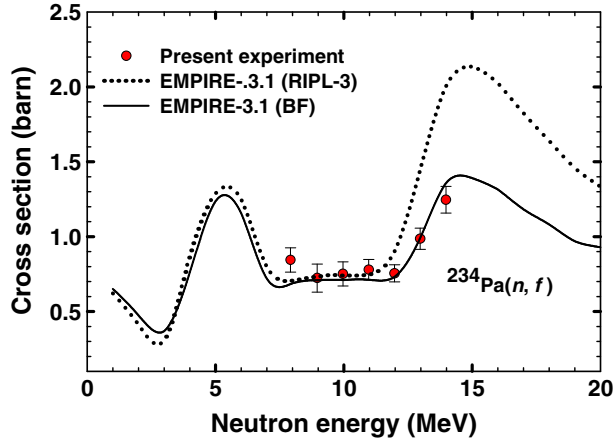
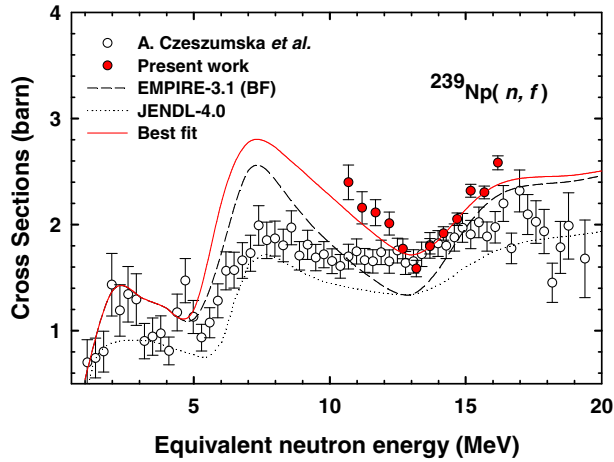


Figure 2. Experimental  $^{234}\text{Pa}(n, f)$  cross-sections and calculated results using the EMPIRE-3.1 code (figure taken from [11]).

neutron energies below 12 MeV. For the neutron bombarding energies above 12 MeV, the EMPIRE-3.1 calculations for RIPL-3 overpredict the experimental data.

#### 4. Determination of $^{239}\text{Np}(n, f)$ and $^{240}\text{Np}(n, f)$ cross-sections

The  $^{238}\text{U}(^6\text{Li}, \alpha f)^{240}\text{Np}^*$  (surrogate of  $n+^{239}\text{Np} \rightarrow ^{240}\text{Np}^*$ ) and  $^{238}\text{U}(^6\text{Li}, df)^{242}\text{Pu}^*$  (surrogate of  $n+^{241}\text{Pu} \rightarrow ^{242}\text{Pu}^*$ ) transfer reactions at  $E_{\text{lab}} = 39.6$  MeV have been used to produce  $^{240}\text{Np}^*$  and  $^{242}\text{Pu}^*$  compound nuclei at an overlapping excitation energy in the range of 16.5–22.5 MeV. The ratios of fission decay probabilities  $P_f^{240}\text{Np}(E_{\text{ex}})/P_f^{242}\text{Pu}(E_{\text{ex}})$  of the compound systems  $^{240}\text{Np}$  and  $^{242}\text{Pu}$  have been determined in steps of 1.0 MeV energy bin. Similarly,  $^{238}\text{U}(^7\text{Li}, \alpha)^{241}\text{Np}$  (surrogate of  $n+^{240}\text{Np} \rightarrow ^{241}\text{Np}$ ) and  $^{238}\text{U}(^7\text{Li}, t)^{242}\text{Pu}$  (surrogate of  $n+^{241}\text{Pu} \rightarrow ^{242}\text{Pu}$ ) transfer reactions at  $E_{\text{lab}} = 41$  MeV have been used to populate  $^{241}\text{Np}$  and  $^{242}\text{Pu}$  compound nuclei at the overlapping excitation energy in the range of 15.0–22.0 MeV. The ratios of fission decay probabilities  $P_f^{241}\text{Np}(E_{\text{ex}})/P_f^{242}\text{Pu}(E_{\text{ex}})$  of the compound systems  $^{241}\text{Np}$  and  $^{242}\text{Pu}$  have been determined in 1.0 MeV excitation energy bin. The ratios of fission decay probabilities  $P_f^{240}\text{Np}(E_{\text{ex}})/P_f^{242}\text{Pu}(E_{\text{ex}})$  and  $P_f^{241}\text{Np}(E_{\text{ex}})/P_f^{242}\text{Pu}(E_{\text{ex}})$  are then multiplied by the ratio of the corresponding neutron-induced compound nucleus formation cross-section,  $\sigma_{n+^{239}\text{Np}}^{\text{CN}}(E_{\text{ex}})/\sigma_{n+^{241}\text{Pu}}^{\text{CN}}(E_{\text{ex}})$  and  $\sigma_{n+^{240}\text{Np}}^{\text{CN}}(E_{\text{ex}})/\sigma_{n+^{241}\text{Pu}}^{\text{CN}}(E_{\text{ex}})$  to obtain the compound nuclear reaction cross-section ratios  $\sigma_f^{n+^{239}\text{Np} \rightarrow ^{240}\text{Np}}(E_{\text{ex}})/\sigma_f^{n+^{241}\text{Pu} \rightarrow ^{242}\text{Pu}}(E_{\text{ex}})$  and  $\sigma_f^{n+^{240}\text{Np} \rightarrow ^{241}\text{Np}}(E_{\text{ex}})/\sigma_f^{n+^{241}\text{Pu} \rightarrow ^{242}\text{Pu}}(E_{\text{ex}})$  at similar excitation energies using eq. (1). The neutron-induced compound nucleus formation cross-sections for the present reactions have been determined using the EMPIRE-3.1 code. The  $\sigma_f^{n+^{241}\text{Pu}}$  cross-section values as function of excitation energy are used as the reference, which have been derived from Tovesson and Hill [19] using the neutron



**Figure 3.** Experimental  $^{239}\text{Np}(n, f)$  cross-sections, present measurements (solid circles), and the work of Czeszumska *et al* [20] (open circles). Calculated results are from the EMPIRE-3.1 code for fission barrier parameters obtained from BF (short dashed line). The adopted data from the JENDL-4.0 [19] nuclear data library (dotted line) and the best fit (solid line) are also shown (figure taken from [10]).

separation energy of  $^{242}\text{Pu}$  ( $S_n = 6.545$  MeV). The  $^{239}\text{Np}(n, f)$  and  $^{240}\text{Np}(n, f)$  cross-sections as functions of excitation energy were obtained over the excitation energy ranges of 16.5–22.5 and 15–22 MeV, respectively, using eq. (1). The  $^{239}\text{Np}(n, f)$  and  $^{240}\text{Np}(n, f)$  cross-sections as functions of excitation energy are then converted to the equivalent neutron energy ranges of 10.5–16.5 and 9.0–16.0 MeV by using neutron separation energies

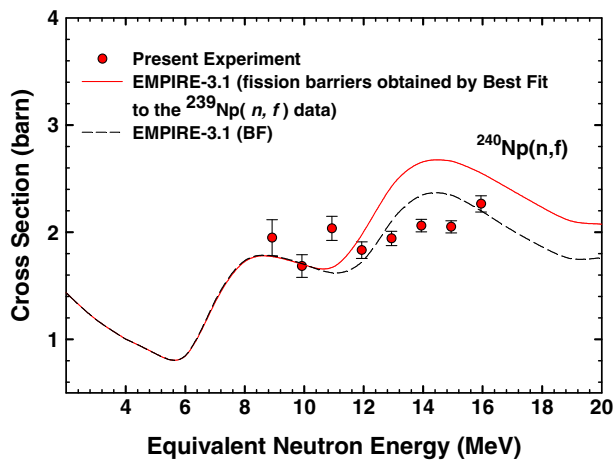


**Figure 4.** Experimental  $^{240}\text{Np}(n, f)$  cross-sections and calculated results using the EMPIRE-3.1 code (figure taken from [10]).

of  $^{240}\text{Np}$  ( $S_n = 5.07$  MeV) and  $^{241}\text{Np}$  ( $S_n = 6.13$  MeV), respectively. The present experimental data have been compared with the recently reported  $^{239}\text{Np}(n, f)$  cross-sections by Czeszumaska *et al* [20], and the adopted cross-section data from JENDL-4.0 [21] are shown in figure 3 along with the calculated cross-sections using the EMPIRE-3.1 code for fission barrier parameters obtained from BF. The present experimental results for the  $^{239}\text{Np}(n, f)$  cross-sections are found to be somewhat higher than the predictions of the EMPIRE-3.1 code. It can also be seen from figure 3 that the  $^{239}\text{Np}(n, f)$  cross-sections of this work closely follow the recently reported  $^{239}\text{Np}(n, f)$  cross-sections by Czeszumaska *et al* [20] in the neutron energy range of 13.0–16.0 MeV; however, the  $^{239}\text{Np}(n, f)$  cross-section values deduced by Czeszumaska *et al* [20] in the neutron energy range of 10.0–13.0 MeV are different from the present results. The trend of the JENDL-4.0 data is much lower compared to the present values of experimental  $^{239}\text{Np}(n, f)$  cross-sections. However, it is observed that, by reducing the inner and outer barrier heights of the  $^{239}\text{Np}$  isotope from the BF-predicted values of 5.84 and 5.56 MeV to 5.10 and 5.25 MeV, respectively, a better comparison with the present experimental  $^{239}\text{Np}(n, f)$  cross-sections data with the EMPIRE-3.1 code calculations is obtained, as shown in figure 3 and denoted as ‘best fit’. The present experimental  $^{240}\text{Np}(n, f)$  cross-sections are found to compare reasonably well with the EMPIRE-3.1 calculations in the neutron energy range of 9.0–16.0 MeV, as shown in figure 4, for default BF barrier parameters and also for the best fit of  $^{239}\text{Np}(n, f)$  barriers.

## 5. Summary and conclusions

In summary, we have employed a new surrogate approach, which involves aspects of both absolute and surrogate ratio method, in a unique way to determine the  $^{234}\text{Pa}(n, f)$ ,  $^{239}\text{Np}(n, f)$ , and  $^{240}\text{Np}(n, f)$  cross-sections using  $^7\text{Li} + ^{232}\text{Th}$  and  $^6,7\text{Li} + ^{238}\text{U}$  transfer fission coincidence measurements. The present experimental data have been compared with the predictions of EMPIRE-3.1 for fission barrier parameters corresponding to RIPL-3 and barrier formula. This work demonstrated the use of surrogate reaction method to determine neutron-induced fission cross-sections for unstable actinide targets relevant for nuclear energy applications.

## References

- [1] J E Escher, J T Burke, F S Dietrich, N D Scielzo, I J Thompson and W Younes, *Rev. Mod. Phys.* **84**, 353 (2012)
- [2] J D Cramer and H C Britt, *Phys. Rev. C* **2**, 2350 (1970)
- [3] H C Britt and J D Cramer, *Phys. Rev. C* **2**, 1758 (1970)
- [4] M S Basunia *et al*, *Nucl. Instrum. Methods B* **267**, 1899 (2009)
- [5] C Plettner *et al*, *Phys. Rev. C* **71**, 051602(R) (2005)
- [6] J T Burke *et al*, *Phys. Rev. C* **73**, 054604 (2006)
- [7] V V Desai, B K Nayak, A Saxena, D C Biswas, E T Mirgule, Bency John, S Santra, Y K Gupta, L S Danu, G K Prajapati *et al*, *Phys. Rev. C* **87**, 034604 (2013)

- [8] J J Ressler *et al*, *Phys. Rev. C* **83**, 054610 (2011)
- [9] B K Nayak *et al*, *Phys. Rev. C* **78**, 061602(R) (2008)
- [10] V V Desai, B K Nayak, A Saxena, E T Mirgule and S V Suryanarayana, *Phys. Rev. C* **88**, 014613 (2013)
- [11] V V Desai, B K Nayak, A Saxena and E T Mirgule, *Phys. Rev. C* **89** (2014)
- [12] B F Lyles *et al*, *Phys. Rev. C* **78**, 061602(R) (2008)
- [13] M B Chadwick *et al*, *Nucl. Data Sheets* **107**, 2931 (2006)
- [14] M Herman *et al*, *Nucl. Data Sheets* **108**, 2655 (2007)
- [15] R Capote *et al*, *J. Nucl. Sci. Tech. (Japan)* **45**, 333 (2008)
- [16] S K Gupta and A Saxena, in *Proceedings of 8th International Workshop on Nuclear Data Production and Evaluation (NDPE)*, Pohang Accelerator Laboratory (PAL) (Pohang University of Science and Technology (POSTECH), Korea, 2005)
- [17] S K Gupta and L Satpathy, *Z. Phys. A* **326**, 221 (1987)
- [18] R Capote *et al*, *Nucl. Data Sheets* **110**, 3107 (2009)
- [19] F Tovesson and T S Hill, *Nucl. Sci. Eng.* **165**, 224 (2010)
- [20] A Czeszumska *et al*, *Phys. Rev. C* **87**, 034613 (2013)
- [21] K Shibata *et al*, *J. Nucl. Sci. Technol.* **48**, 1 (2011)